

Fig. 2 shows the hydraulic scheme and the equivalent electric circuits of a surge tank. The piezometric heads H and the flow rates Q on the hydraulic side are replaced on the electric side by voltages and currents. All the elements of the equivalent electrical circuits can be deduced from the hydraulic parameters. This procedure can be used for each hydraulic component as explained in [3]. Only the case of a pipe segment will be briefly described in this paper.

In the case of a pipe segment, the electric equivalent circuit can be obtained using the momentum and mass conservation equations:

$$\frac{\partial H}{\partial x} + \underbrace{\frac{1}{gA}}_{L'} \frac{\partial Q}{\partial t} + \underbrace{\frac{\lambda|Q|}{2gDA^2}}_{R'} Q = 0 \quad (1)$$

$$\frac{\partial H}{\partial t} + \underbrace{\frac{a^2}{gA}}_{1/C'} \frac{\partial Q}{\partial x} = 0 \quad (2)$$

with:

- A = cross section [m²]
- λ = friction factor
- D = pipe diameter [m]
- a = wave speed [m/s]

L' [s²/m³], C' [m], R' [s/m³] = hydro acoustic linear inductance, capacity, resistance

Equations (1) and (2) become the telegraphic equations (3) of an electrical transmission line if the piezometric head H and the flow rate Q are replaced by the voltage U and the current I :

$$\begin{aligned} \frac{\partial U}{\partial x} + L_e \frac{\partial I}{\partial t} + R_e I &= 0 \\ \frac{\partial U}{\partial t} + \frac{1}{C_e} \frac{\partial I}{\partial x} &= 0 \end{aligned} \quad (3)$$

L_e [H/m], C_e [F/m], R_e [Ω /m] = linear inductance, capacity, resistance.

A pipe must always be divided into a series of N elementary pipe segments with the length dx ; in that respect it is necessary to reformulate the equations (1) and (2) by choosing as state variables the piezometric head in the middle of the segment $H_{i+1/2}$ and the input / output flow rates Q_i / Q_{i+1} . The input / output piezometric heads H_i / H_{i+1} become boundary conditions for this pipe segment. The first derivatives of H and Q in the middle of the pipe element i can be written according to Fig. 3:

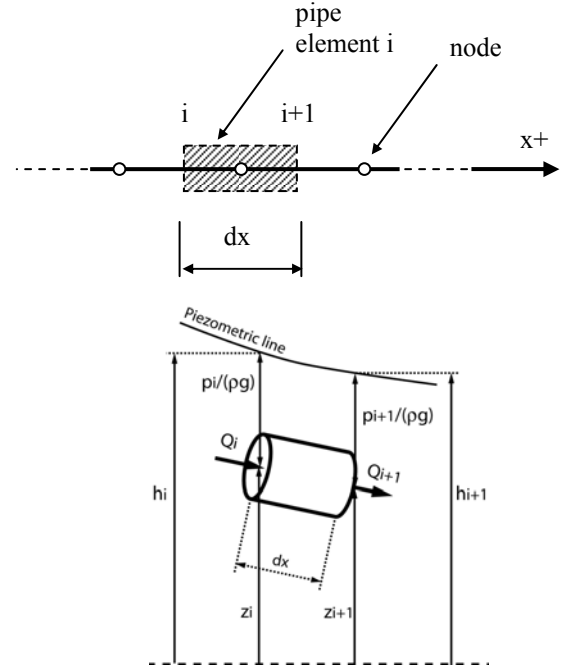


Fig.3: Discretization of a pipe into n elements

$$\left. \frac{\partial H}{\partial x} \right|_{i+1/2} = \frac{H_{i+1} - H_i}{dx} \quad (4)$$

$$\left. \frac{\partial Q}{\partial x} \right|_{i+1/2} = \frac{Q_{i+1} - Q_i}{dx} \quad (5)$$

Using these derivatives, equations (1) and (2) take the form:

$$\frac{dH_{i+1/2}}{dt} + \frac{1}{C'} \cdot \frac{Q_{i+1} - Q_i}{dx} = 0 \quad (6)$$

$$\frac{H_{i+1} - H_i}{dx} + L' \cdot \frac{dQ_{i+1/2}}{dt} + R' \cdot Q_{i+1/2} = 0 \quad (7)$$

$$\text{with: } Q_{i+1/2} = \frac{Q_{i+1} + Q_i}{2}$$

the equations (6) and (7) become:

$$C' \cdot dx \cdot \frac{dH_{i+1/2}}{dt} = -(Q_{i+1} - Q_i) \quad (8)$$

$$\begin{aligned} H_{i+1} + \underbrace{\frac{L' \cdot dx}{2} \cdot \frac{dQ_{i+1}}{dt} + \frac{R' \cdot dx}{2} \cdot Q_{i+1}}_{H_{i+1/2}} = \\ H_i - \underbrace{\left(\frac{L' \cdot dx}{2} \cdot \frac{dQ_i}{dt} + \frac{R' \cdot dx}{2} \cdot Q_i \right)}_{H_{i+1/2}} \end{aligned} \quad (9)$$

$R = R'.dx$; $L = L'.dx$; $C = C'.dx$, equations (8) and (9) lead to the electrical equivalent circuit given in Fig. 4, which can be used in the SIMSEN electric version for modelling a pipe segment.

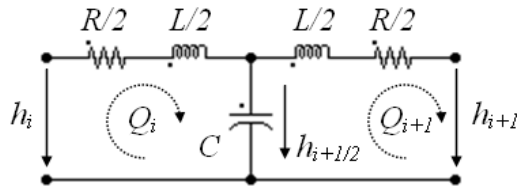


Fig.4: Electrical equivalent circuit of a pipe segment

This procedure can be used to define an equivalent electrical circuit for each hydraulic component (valve, surge tank, pump turbine ...) [2].

III APPLICATIONS

The simulation of the transient behavior of the power plant of Fig. 5 is performed for 2 cases:

- A: load acceptance, short circuit and shutdown;
- B: load rejection in islanded power network.

The main hydraulic data of the power plant in Fig. 5 are given in Table 1.

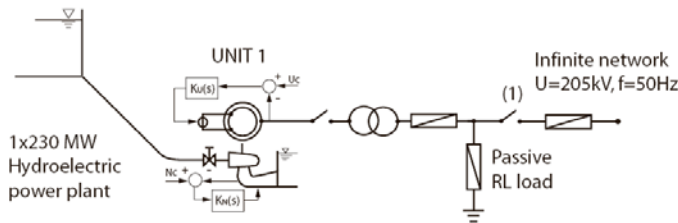


Fig. 5: Layout of the hydroelectric power plant

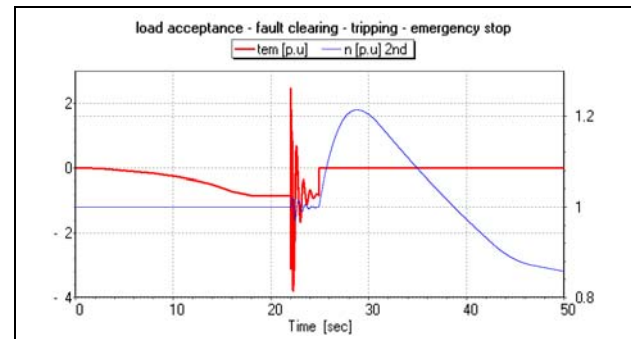
Table 1: Main data of the power plant.

Main data of the power plant			
Reservoir	Penstock	Turbine	Generator
$H_0=315\text{m}$	$L=1100\text{ m}$ $D=5\text{ m}$ $\lambda=0,02$ $a=1100\text{ m/s}$	$H_n=309\text{ m}$ $Q_n=85,3\text{ m}^3/\text{s}$ $T_n=5,85 \cdot 10^6\text{ Nm}$ $J_t=5 \cdot 10^4\text{ kg}\cdot\text{m}^2$	$S_n=250\text{MVA}$ $U_n=17,5\text{ kV}$ $F_n=50\text{ Hz}$ $J_g=1 \cdot 10^6\text{ kg}\cdot\text{m}^2$
Initial load conditions			
Element	Active Power	Reactive Power	
Generator	$P=-200\text{ MW}$	$Q=-100\text{MVar}$	
Passive Load	$P=150\text{ MW}$	$Q=50\text{MVar}$	
Network	$P=50\text{ MW}$	$Q=50\text{MVar}$	

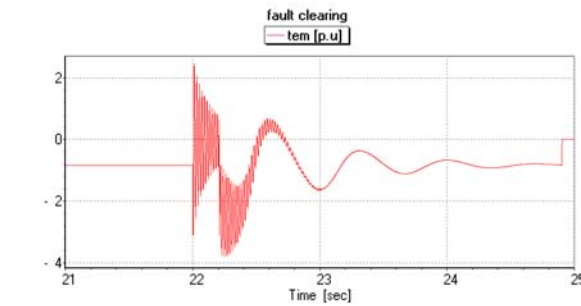
A. Load acceptance, short-circuit and shutdown

Fig. 6 illustrates the behavior of the power plant during the first application including the following operation steps:

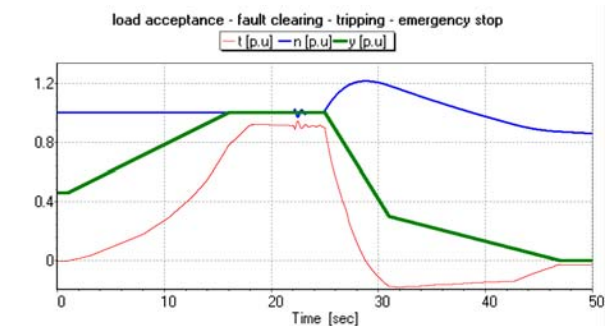
- Initial conditions: unit connected to the network under no-load operation during 1 s.



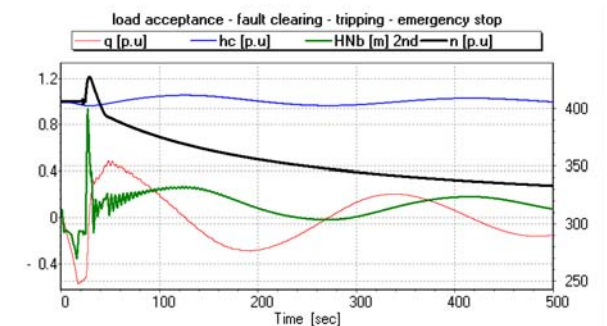
a) Electromagnetic torque tem and speed n of the hydro-generator



b) Electromagnetic torque during 3 phase fault and fault clearing



c) turbine torque t, speed n, turbine guide vane opening y



d) surge tank inlet discharge q, surge tank level hc, turbine inlet piezometric head HNb, speed n

Fig. 6: Numerical simulation of a hydroelectric production site under transient conditions.

- Turbine guide vane opening in 15 s, load acceptance.
- Steady-state operation since $t = 16$ s.
- At $t = 22$ s: 3 phase fault occurs on the HV side of the transformer with successful fault clearing 200 ms later.
- At $t = 24,9$ s the circuit breaker of the unit is switched off, tripping of the unit.
- At $t = 25$ s the turbine emergency closure is switched on.

The analysis of the results given in Fig. 6 leads to the following remarks:

- The 3 phase short-circuit on the HV side of the transformer unit and its clearing 200 ms later represent strong constraints for the electric part of the configuration (Fig. 6b), however they have no significant influence on the hydraulic quantities.
- As expected the constraints acting on the hydraulic components are most severe during the turbine emergency closure (Fig. 6d), the turbine inlet piezometric head increase exceeds 40%.
- The surge tank is properly taken into account; the time variations of the surge tank inlet discharge q and of the level h_c can be seen clearly in magnitude and phase in Fig. 6d.
- The long time simulation in Fig. 6d shows the low frequency mass oscillation in the surge tank compared to the pulsating component of the turbine inlet piezometric head due to the waterhammer effect.

B. Load rejection in islanded power network

The second application concerns also the hydroelectric power plant represented in Fig. 5. For this application the installation is driven by a turbine speed governor and a generator voltage regulator. Both are of the PID type.

The transient behaviour investigated is the network load rejection. This is done by switching off the circuit breaker (1) at $t = 10$ s. Two different models are compared:

(i) - Hydroelectric model according to Fig. 5: the synchronous generator is going into an islanded operation after the circuit breaker switching off. The active and reactive loads are reduced by 25, respectively 50%.

(ii)- Hydraulic model: the generator and the electrical network are simply modelled by a counter torque reduced by 25 % at $t = 10$ s.

The simulation results of this 25% active load rejection obtained with the hydraulic and the hydroelectric models are illustrated in Fig. 7 top and bottom. The time evolution of the referred head H/H_n , discharge Q/Q_n , rotational speed N/N_n , torque T/T_n , guide vane opening y and electromagnetic torque T_{el}/T_n are represented. It can be seen that the simulation results obtained using the hydraulic model is fully stable, the stability is recovered 40s after the disturbance. However, using the same turbine speed governor settings with the hydroelectric model, a dynamic response at the limit of stability of the system is obtained. After 90s, the system still not recovers stable operating conditions. This difference is due to the strong dynamic influence of the electrical part of the installation in the islanded production mode. It can be seen

by comparing the electromagnetic torques T_{el}/T_n obtained with both models.

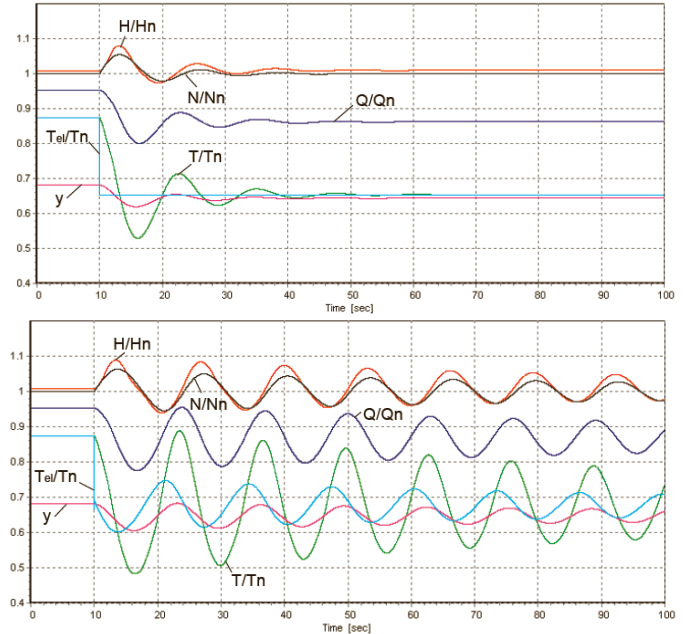


Fig. 7: Simulation results of the transient of the Francis turbine resulting from a 25% load rejection with the hydraulic model (top) and the hydroelectric model (bottom).

This means, that for islanded production modes, the set of parameters of a turbine speed governor cannot be determined with only a simple hydraulic model not taking into account the electrical equipment.

In order to deeply analyze both models, the transfer function of the turbine $G(s)$ is identified using a numerical simulation. The guide vane opening y is the input variable and the turbine rotational speed N is the output variable. The transfer function of the turbine $G(s)$ is expressed in the Laplace domain as follows:

$$G(s) = N(s) / Y(s)$$

A PRBS signal (pseudorandom binary signal) of 2% amplitude is superimposed on the mean value of the guide vane opening y for the identification of the transfer function $G(s)$. From the time domain simulation the time evolution of the rotational speed and of the guide vane opening are used for the calculation of the transfer function of each model. The comparison in Fig. 8 between the two transfer functions obtained leads to the following remarks:

- The natural frequencies of the mechanical inertias are present at 3.5 Hz and 16.3 Hz. The lowest one is an anti-resonance of the generator inertia while the second one is the resonance of the turbine inertia.

- The odd eigen frequencies of the penstock are also present for $f = 0.25, 0.75, 1.25$ Hz and so on, corresponding respectively to $f = a/(4L), 3a/(4L), 5a/(4L)$, and so on, up to the 20th eigen frequency for a penstock model with 20 nodes.

- The two transfer functions are almost identical except for very low frequencies where the amplitudes of the

hydroelectric transfer function are much higher than those of the hydraulic transfer function. These high amplitudes result from the dynamics of the electrical network in the islanded production mode. This difference at very low frequencies restricts the performances of the turbine governor.

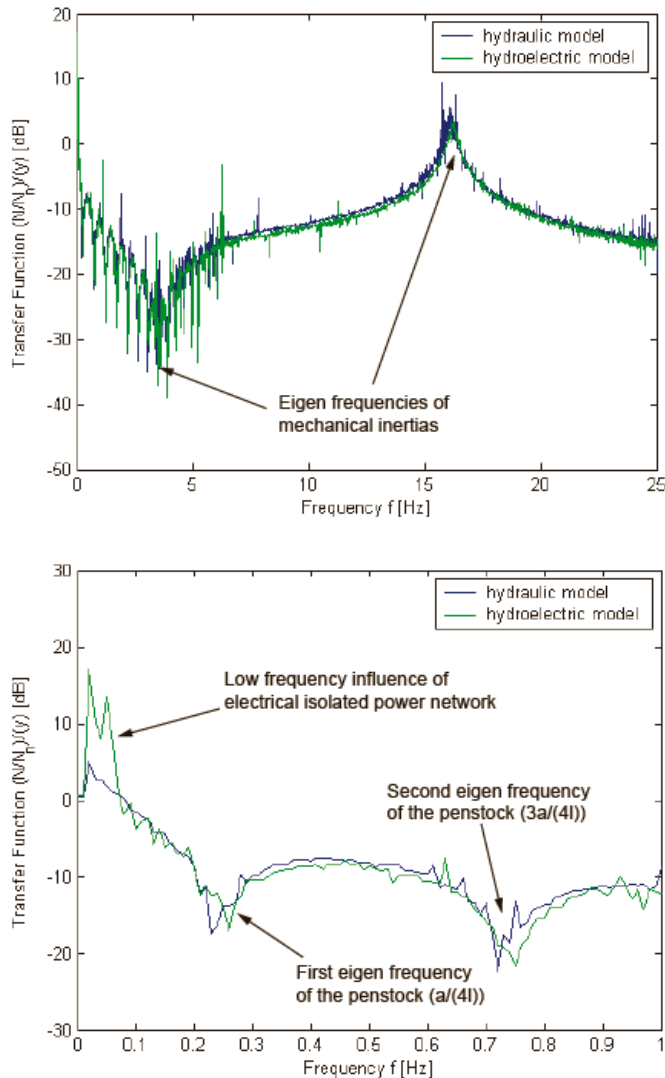


Fig. 8: Transfer function of the turbine $G(s) = N(s)/Y(s)$ in the range 0 – 25 Hz (top) and 0 – 1 Hz (bottom).

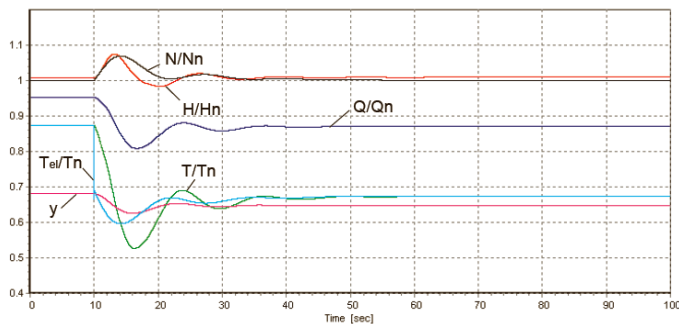


Fig. 9: Simulation results load rejection with the hydroelectric model and the modified integration time constant of the turbine speed governor.

As consequence and in order to be stable in the hydroelectric production mode, the integrator time constant T_i of the PID turbine speed governor is increased to reduce the amplification at low frequencies. The initial integration time constant $T_i = 3.7$ s is increased to $T_i = 14$ s in order to have an efficient governor. The gain and the derivative time constant remain unchanged ($K_p = 1$, $T_d = 1.21$ s). The simulation results of the dynamic behaviour of the installation resulting from a 25% load rejection using the hydroelectric model is presented in Fig 9. It can be seen that, as expected, the system is again fully stable in the islanded production mode.

IV CONCLUSIONS

A numerical software package initially developed for the simulation of electrical power systems and adjustable speed drives has been extended to the hydraulic components of a hydroelectric production site having an arbitrary topology. This new simulation tool is able to take into account all the important interactions between both parts of a hydroelectric production site. It is therefore very useful for stability analysis, especially in case of islanded operation. This new tool can also be used for global design optimization.

REFERENCES

- [1] J.-J. Simond, A. Sapin, M. Tu Xuan, R. Wetter, P. Burmeister, 12-Pulse LCI Synchronous Drive for a 20 MW Compressor - Modeling, Simulation and Measurements - IEEE-IAS Meeting 2005, Hong-Kong.
- [2] C. Nicolet, F. Avellan, Ph. Allenbach, A. Sapin, J.-J. Simond, S. Kvicinsky, M. Crahan, Simulation of transient phenomena in Francis turbine power plants: Hydroelectric interaction. Waterpower XIII 2003, Buffalo.
- [3] C. Nicolet, F. Avellan, Ph. Allenbach, A. Sapin, J.-J. Simond, New Tool for the Simulation of Transient Phenomena in Francis Turbine Power Plants. IAHR Symposium 2002.
- [4] C. Nicolet, B. Greiveldinger, J.-J. Hérou, P. Allenbach, J.-J. Simond, F. Avellan, On the Hydroelectric Stability of an Islanded Power Network: IEEE – PES Annual Meeting, June 2006, Montreal.